

## INTRODUCTION TO DIFFUSE INTERFACES AND TRANSFORMATION FRONTS MODELLING IN COMPRESSIBLE MEDIA

RICHARD SAUREL<sup>1,2</sup> AND FABIEN PETITPAS<sup>1,2</sup>

**Abstract.** Computation of interfaces separating compressible materials is related to mixture cells appearance. These mixture cells are consequences of fluid motion and artificial smearing of discontinuities. The correct computation of the entire flow field requires perfect fulfillment of the interface conditions. In the simplest situation of contact interfaces with perfect fluids, these conditions correspond to equal normal velocities and equal pressures. To compute compressible flows with interfaces two main classes of approaches are available. In the first one, the interface is considered as a sharp discontinuity. Lagrangian, Front Tracking and Level Set methods belong to this class. The second option consists in the building of a flow model valid everywhere, in pure materials and mixture cells, solved routinely with a unique Eulerian algorithm [37]. In this frame, the interface is considered as a numerically diffused zone, captured by the algorithm. There are some advantages with this approach, as the corresponding flow model is not only valid in artificial mixture cells, but it also describes accurately true multiphase mixtures of materials.

The [37] approach has been simplified by [22] with the help of asymptotic analysis, resulting in a single velocity, single pressure but multi-temperature flow model. This reduced model presents however difficulties for its numerical resolution as one of the equations is non-conservative. In the presence of shocks, jump conditions have been provided by [42], determined in the weak shock limit. When compared against experiments for both weak and strong shocks, excellent agreement was observed. These relations have been accepted as closure shock relations for the [22] model and allowed the study of detonation waves in heterogeneous energetic materials. Generalized Chapman-Jouguet conditions were obtained as well as heterogeneous explosives (non-ideal) detonation wave structures [36].

Oppositely to the previous example of exothermic reactions and high speed flows, endothermic reactions are considered in [43] to deal with cavitating and flashing flows. In conjunction with capillary [33] and diffusive effects, it has been possible to deal with boiling flows [25].

Extra multiphysic extensions such as dynamic powder compaction [38], solid-fluid coupling in extreme deformations [12] have been investigated too.

---

<sup>1</sup> Aix-Marseille Université, CNRS, IUSTI UMR 7343, 5 rue E. Fermi, 13453, Marseille, France

<sup>2</sup> Also, RS2N, Bastidon de la Caou, 13360 Roquevaire, France

**Résumé.** La résolution numérique des problèmes à interfaces entre milieux compressibles est fortement liée à l'apparition de 'maillages de mélange'. Celles-ci sont liées au mouvement des fluides sur maillages fixes, induisant une diffusion artificielle des discontinuités de contact. La résolution numérique de l'ensemble de l'écoulement nécessite le respect des conditions d'interface, qui correspondent pour les fluides parfaits à l'égalité des vitesses normales et à l'égalité des pressions.

Pour résoudre les écoulements de fluides compressibles en présence d'interfaces matérielles, essentiellement deux catégories de méthodes sont disponibles. Dans la première catégorie, l'interface est considérée comme une discontinuité. Les méthodes lagrangiennes, de 'suivi de front' et Level Set appartiennent à cette catégorie. La seconde option consiste en la construction d'un modèle d'écoulement valide partout, dans les milieux purs ainsi que dans les zones de mélange, résolu routinièrement avec un unique solveur eulérien [37]. Dans ce contexte, les interfaces sont traitées en tant que zones de diffusion numérique, capturées par l'algorithme. Cette approche présente certains avantages. Par exemple, le modèle d'écoulement n'est pas seulement valable dans les maillages de mélange artificiel, mais aussi dans les zones d'écoulement diphasiques d'origine physique et ayant des évolutions hors d'équilibre.

L'approche de [37] a été simplifiée par [22] sur la base d'une analyse asymptotique dans la limite de forts coefficients de relaxation des vitesses et des pressions. Cette analyse conduit à un modèle à une seule vitesse et une seule pression, mais en déséquilibre de températures. La résolution numérique de ce modèle présente néanmoins certaines difficultés, en raison du caractère non conservatif d'une des équations. En présence d'ondes de choc, des relations de saut ont été proposées [42] et justifiées dans la limite des chocs faibles. Ces relations ont été validées par rapport à toutes les expériences disponibles, à la fois pour les chocs faibles et forts. Elles ont donc été acceptées comme relations de fermeture aux chocs pour le modèle de [22] et ont permis l'étude des ondes de détonation dans les matériaux énergétiques hétérogènes. Des conditions de Chapman-Jouguet généralisées ont été obtenues ainsi que la structure des ondes de détonation correspondantes (non idéales) [36].

A l'opposé des situations précédentes de transformations exothermiques dans des écoulements à grandes vitesses, des réactions d'évaporation endothermiques ont été considérées [43] pour traiter les écoulements cavitants et l'évaporation 'flash'. Lorsque cette modélisation de la transition de phase est combinée aux effets capillaires [33] et diffusifs, il est possible de traiter la simulation numérique directe de l'ébullition nucléée [25].

Enfin, d'autres extensions sont aussi envisageables, telles que la compaction dynamique des poudres [38] ou le couplage solide-fluide en déformations extrêmes [12].

## INTRODUCTION

The computation of interfaces and waves dynamics with compressible materials has many fundamental and industrial applications, ranging from fluid mechanics and astrophysics to chemical, mechanical and environmental engineering. When dealing with compressible materials the main issue is related to the appearance of mixture cells. These mixture cells are consequences of fluid motion and artificial smearing of discontinuities. The correct computation of the entire flow field requires perfect fulfillment of the interface conditions. In the simplest situation of contact interfaces with perfect fluids, these conditions correspond to equal normal velocities and equal pressures. To compute compressible flows with interfaces two main classes of approaches are available. In the first one, the interface is considered as a sharp discontinuity. To avoid as far as possible interface numerical smearing several options are possible:

- Lagrangian and ALE methods (see for example [11, 19]). In this context, the computational mesh moves and distorts with the material interface. However, when dealing with fluid flows, deformations are unbounded and resulting mesh distortions may result in computational failure [45].
- Interface Reconstruction methods use a fixed mesh with an additional equation for tracking and reconstructing the material interface. In the volume of fluid (VOF) approach [20], each computational cell is assumed to possibly contain a mixture of fluids and the volume occupied by each fluid is represented

by the volume fraction, transported by the flow. This method is widely used for incompressible flows as there is no thermodynamics to compute in mixture cells [17]. For compressible flows, extra energy equations are used as well as pressure relaxation procedures [4,29]. Multiphase flow ingredients are used with these methods that come quite close to the diffuse interface methods discussed later.

- Level-Set methods [30,31,47] are very popular methods to spatially locate interfaces. Special management of the interfaces is needed to preserve jump conditions. Relevant work in this direction was done by [13] with the Ghost Fluid Method.
- Front Tracking methods consider explicit interface tracking over a fixed Eulerian mesh [15,27].

With the various preceding methods, the interface is managed with a specific treatment, having consequences with respect to coding complexity, conservation issues, extra physics extension capabilities and robustness especially in severe conditions. The second class of approaches follows another philosophy, closer to the one of capturing methods. Capturing methods are fundamental contributions of [52] and [16]. The aim was to solve the same equations with the same numerical scheme in both smooth and discontinuous flow regions. Pioneer works in 'interface capturing' or 'diffuse interfaces' modelling areas were done about forty years latter by [23]. Indeed, interfaces computation posed extra difficulties linked to thermodynamic state computation in artificial mixture zones. Determination of thermodynamic flow variables in these mixture zones has been achieved on the basis of multiphase flow modelling by [37]. Some advantages appeared:

- As already mentioned, the same equations are solved everywhere (interfaces, shocks, expansions waves) with a unique flow solver.
- These models and methods are able to dynamically create interfaces (not present initially) as for example in cavitating flows [41,43].
- These methods are also able to deal with interfaces separating pure fluids and fluid mixtures, as for example when a granular material is in contact with a fluid [9,38].
- As this approach includes the two velocities flow model of [2] it is also possible to compute velocity non-equilibrium bubbly or granular flows in conjunction with material interfaces [14,39].

In the same period of time, a reduced model has been built by [22]. Here, pressure and velocity equilibrium is assumed, rendering the resulting model unable to deal with velocity non-equilibrium mixtures, but resulting in a more appropriate model for interface computations.

As it is more convenient to add extra physics in a single velocity context, multiphysics capabilities have been considered in the [22] framework. Surface tension modelling [33], shock and detonation computation in heterogeneous materials [36,42], phase transition [43], elastic solid - fluid coupling [12], powder compaction [38], interpenetration effects at unstable interfaces [40] are examples of such extensions.

To summarize, diffuse interface modelling allows quite advanced multiphysics extensions still solving a unique set of hyperbolic partial differential equations with a unique Godunov type flow solver.

The aim of the present paper is not to summarize all these possible extensions but to give a comprehensive introduction to the 'diffuse interface' approach. To do this, Section 1 presents a hyperbolic non-equilibrium two-phase flow model that is a good starting point to describe natural or artificial two-phase mixtures. The [22] model is presented in Section 2 as a reduced version of the previous non-equilibrium model. This model is the simplest candidate for diffuse interface modelling with non-barotropic fluids. The [22] model being non conservative, shock relations have to be determined as well as appropriate numerical schemes. The [42] shock relations are presented in the same section and the relaxation algorithm of [44] is summarized in Section 3. Some extensions are then presented. First, in Section 4 with capillary effects. Second in Section 5 with phase transition modelling and last with detonation modelling in Section 6. Section 7 deals with open issues, such as low Mach number flows with diffuse interface models, diffuse interfaces sharpening and extra multiphysics extensions.

## 1. TOTAL DISEQUILIBRIUM MIXTURES

The [22] model we are going to use for the various multiphysics extensions comes from a more general model, out of mechanical, thermal and chemical equilibrium. The non-equilibrium mixture model presented hereafter consists in a symmetric formulation of the [2] model developed in [39]:

$$\left\{ \begin{array}{l} \frac{\partial \alpha_1}{\partial t} + u_I \frac{\partial \alpha_1}{\partial x} = \mu(p_1 - p_2), \\ \frac{\partial \alpha_1 \rho_1}{\partial t} + \frac{\partial \alpha_1 \rho_1 u_1}{\partial x} = 0, \\ \frac{\partial \alpha_1 \rho_1 u_1}{\partial t} + \frac{\partial \alpha_1 \rho_1 u_1^2 + \alpha_1 p_1}{\partial x} = p_I \frac{\partial \alpha_1}{\partial x} - \lambda(u_1 - u_2) \\ \frac{\partial \alpha_1 \rho_1 E_1}{\partial t} + \frac{\partial \alpha_1 (\rho_1 E_1 + p_1) u_1}{\partial x} \\ \qquad \qquad \qquad = p_I u_I \frac{\partial \alpha_1}{\partial x} - \lambda u_I' (u_1 - u_2) - p_I' \mu (p_1 - p_2) \end{array} \right. \quad (1)$$

The second phase obeys a symmetrical set of equations.

Notations are conventional:  $\alpha_k, \rho_k, u_k, p_k$  represent respectively the volume fraction, the density, the velocity and the pressure of phase k. The total energy of phase k is defined by  $E_k = e_k + 1/2 u_k^2$ , with  $e_k$  the internal energy of phase k. This model is hyperbolic and fulfills the second law of thermodynamics. The closure relations for the relaxation parameters ( $\mu$  and  $\lambda$ ) as well as for interfacial variables estimates  $u_I, u_I', p_I, p_I'$  are given in the same reference. This model is able to describe two-phase mixtures out of velocity equilibrium. Waves propagation is preserved thanks to the hyperbolic character of the equations and to the presence of relaxation effects. This model can be used for the computation of interface problems with perfect fulfillment of interface conditions. This goal can be reached with two different options:

- The first option consists in using stiff mechanical relaxation parameters  $\mu$  and  $\lambda$  [37].
- The second one is based on non-conservative terms  $u_I \frac{\partial \alpha_1}{\partial x}$  and  $p_I \frac{\partial \alpha_1}{\partial x}$  [1].

The first method is simple and robust. The second one is more subtle but renders possible the consideration of zones out of velocity equilibrium in conjunction with macroscopic interfaces where normal velocities and pressures have to be equal. In particular, it is able to deal with bubbles clouds crossing through material interfaces.

Consideration of extra physics in this formulation is possible but easier in the framework of single velocity formulations. The rest of this paper places in this context, as single velocity models are suitable for many applications.

## 2. MECHANICAL EQUILIBRIUM MODEL, DIFFUSE INTERFACES

The [22] model is obtained as zero order asymptotic limit of the previous model in the limit of relaxation parameters  $\mu$  and  $\lambda$  tending to infinity. Therefore it corresponds to the first option mentioned previously with

the non-equilibrium model and stiff mechanical relaxation. It reads:

$$\left\{ \begin{array}{l} \frac{\partial \alpha_1}{\partial t} + u \frac{\partial \alpha_1}{\partial x} = \alpha_1 \alpha_2 \frac{\rho c_w^2}{\rho_1 c_1^2 \rho_2 c_2^2} (\rho_2 c_2^2 - \rho_1 c_1^2) \frac{\partial u}{\partial x}, \\ \frac{\partial \alpha_1 \rho_1}{\partial t} + \frac{\partial \alpha_1 \rho_1 u}{\partial x} = 0, \\ \frac{\partial \alpha_2 \rho_2}{\partial t} + \frac{\partial \alpha_2 \rho_2 u}{\partial x} = 0, \\ \frac{\partial \rho u}{\partial t} + \frac{\partial \rho u^2 + p}{\partial x} = 0 \\ \frac{\partial \rho E}{\partial t} + \frac{\partial (\rho E + p) u}{\partial x} = 0 \end{array} \right. \quad (2)$$

The total energy is defined as  $E = Y_1 e_1 + Y_2 e_2 + 1/2 u^2$  where  $Y_k = (\alpha_k \rho_k) / \rho$  represent the mass fraction of phase  $k$  and  $\rho = \alpha_1 \rho_1 + \alpha_2 \rho_2$  the mixture density. This model is hyperbolic too with the same wave speeds as the gas dynamic equations but with the [53] sound speed, that presents a non monotonic behaviour with respect to the volume fraction:  $1/(\rho c_w^2) = \alpha_1/(\rho_1 c_1^2) + \alpha_2/(\rho_2 c_2^2)$ . The equation of state allowing the thermodynamic closure is obtained from the mixture energy definition and the pressure equilibrium condition. This equation of state involves at least three arguments:  $p = p(\rho, e, \alpha_1)$ . For example, when each phase obeys the stiffened gas equation of state (see [26] for parameters determination),

$$p_k = (\gamma_k - 1) \rho_k e_k - \gamma_k p_{\infty, k} \quad (3)$$

The mixture equation of state then reads:

$$p(\rho, e, \alpha_1, \alpha_2) = \frac{\rho e - \left( \frac{\alpha_1 \gamma_1 p_{\infty, 1}}{\gamma_1 - 1} + \frac{\alpha_2 \gamma_2 p_{\infty, 2}}{\gamma_2 - 1} \right)}{\frac{\alpha_1}{\gamma_1 - 1} + \frac{\alpha_2}{\gamma_2 - 1}} \quad (4)$$

Parameters  $\gamma_k$  and  $p_{\infty, k}$  are characteristic constants of material  $k$ . As this model involves a single pressure but two mass equations and a volume fraction equation, it is possible to determine two temperatures ( $T_k = T_k(p, \rho_k)$ ) and two entropies. This feature is useful for phase transition modelling.

This model is an excellent candidate for interface problem computations. However, two difficulties at least are present:

- Rankine-Hugoniot relations cannot be determined in a conventional way as the volume fraction equation is non-conservative. With other sets of variables (entropy for example), it is no more possible to obtain meaningful jump conditions.
- The numerical resolution of this model is intricate, due to the presence of the same equation.

The first issue has been considered in [42]. Shock jump conditions have been determined in the weak shock limit. When compared against experimental data of shock speeds in mixtures of materials, for shocks of arbitrary strength (in the megabar range), excellent agreement was obtained. All available data in the Russian

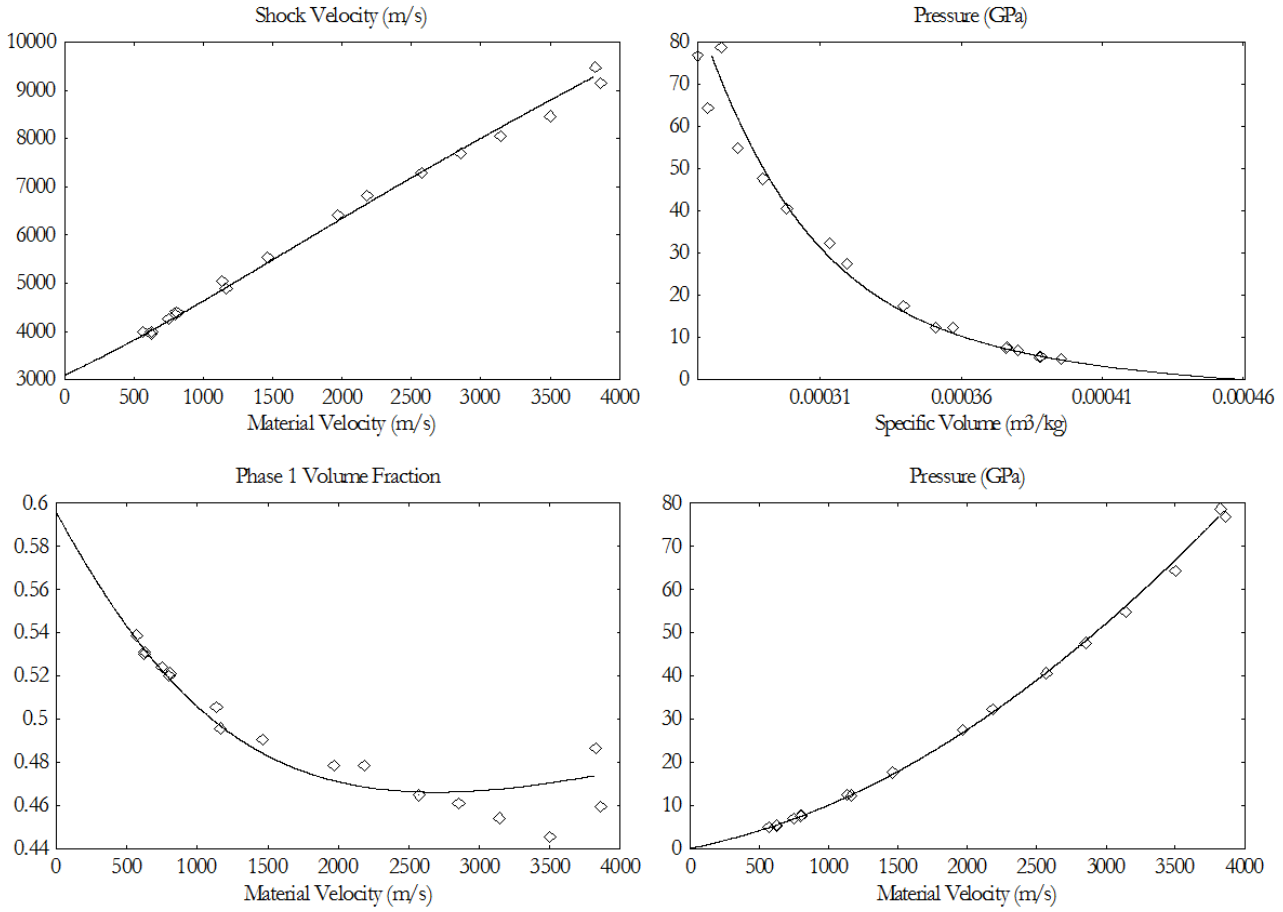


FIGURE 1. Comparison between experiments (symbols) and results obtained from Rankine-Hugoniot relations (5) for the Epoxy-Spinel mixture. Excellent agreement is observed. The same agreement is observed for all mixtures free of phase transition having experimental data in the Russian and American databases.

and American databases have been used in this aim. The corresponding algebraic system reads:

$$\begin{aligned}
 [\alpha_k \rho_k (u - \sigma)] &= 0, & \text{for } k = 1, 2 \\
 [\rho u (u - \sigma) + p] &= 0 \\
 e_k - e_k^0 + \frac{p + p_0}{2} (v_k - v_k^0) &= 0, & \text{for } k = 1, 2 \quad \text{with } v_k = 1/\rho_k
 \end{aligned} \tag{5}$$

A comparison example is given in the Figure 1 for a representative mixture of materials, made of epoxy and spinel. Mixture composition and equations of state parameters are given in [42]. The second difficulty, related to the numerical approximation of System (2) has been addressed in [44] with the strategy summarized in the next section.

### 3. SIMPLE AND EFFICIENT RELAXATION METHOD

To solve System (2), an extended system is considered, that seems more complex at a first glance. However, with this extended system, there is no difficulty to preserve volume fraction positivity. Also, the sound speed with the new model is monotonic with respect to the volume fraction. Last, the Riemann problem resolution is straightforward as will be shown later, as the volume fraction is constant across the right and left facing waves. Nevertheless, to recover solutions of the mechanical equilibrium model (2), stiff pressure relaxation has to be used, preserving volume fraction positivity too. Therefore, the model is solved in a sequence of three steps:

- Solve the extended pressure non-equilibrium flow model, in the absence of relaxation terms, with appropriate hyperbolic solver.
- Relax the pressure toward mechanical equilibrium and determine the volume fraction at pressure equilibrium.
- Compute the pressure with the mixture equation of state (4) based on the relaxed volume fraction and total energy, that results of the additional conservation law (7). Then reset the internal energies with the help of the mixture pressure, phases densities and appropriate equations of state.

Each step is summarized hereafter. The pressure non-equilibrium model reads:

$$\left\{ \begin{array}{l} \frac{\partial \alpha_1}{\partial t} + u \frac{\partial \alpha_1}{\partial x} = \mu (p_1 - p_2), \\ \frac{\partial \alpha_1 \rho_1}{\partial t} + \frac{\partial \alpha_1 \rho_1 u}{\partial x} = 0, \\ \frac{\partial \alpha_2 \rho_2}{\partial t} + \frac{\partial \alpha_2 \rho_2 u}{\partial x} = 0, \\ \frac{\partial \rho u}{\partial t} + \frac{\partial \rho u^2 + \alpha_1 p_1 + \alpha_2 p_2}{\partial x} = 0 \\ \frac{\partial \alpha_1 \rho_1 e_1}{\partial t} + \frac{\partial \alpha_1 \rho_1 e_1 u}{\partial x} + \alpha_1 p_1 \frac{\partial u}{\partial x} = -p_I \mu (p_1 - p_2), \\ \frac{\partial \alpha_2 \rho_2 e_2}{\partial t} + \frac{\partial \alpha_2 \rho_2 e_2 u}{\partial x} + \alpha_2 p_2 \frac{\partial u}{\partial x} = p_I \mu (p_1 - p_2) \end{array} \right. \quad (6)$$

This system can be easily derived from System (1) in the limit of stiff velocity relaxation.

With System (6) combination of the internal energy equations with mass and momentum equations results in the additional mixture energy equation:

$$\frac{\partial \rho \left( Y_1 e_1 + Y_2 e_2 + \frac{1}{2} u^2 \right)}{\partial t} + \frac{\partial \left[ \rho \left( Y_1 e_1 + Y_2 e_2 + \frac{1}{2} u^2 \right) + (\alpha_1 p_1 + \alpha_2 p_2) \right] u}{\partial x} = 0 \quad (7)$$

This extra equation is important during numerical resolution, in order to correct inaccuracies due to the numerical approximation of the non-conservative internal energy equations in the presence of shocks.

This model exhibits a nice feature regarding the mixture sound speed that reads,

$$c_f^2 = Y_1 c_1^2 + Y_2 c_2^2$$

and has a monotonic behaviour versus volume and mass fractions. It represents the frozen mixture speed of sound with respect to the pressure relaxation effects. The model is thus hyperbolic with waves speeds:  $u + c_f$ ,  $u - c_f$  and  $u$ .

System (6) is aimed to replace direct resolution of System (2) by the three steps method mentioned previously. During the first step, System (6) is solved in absence of relaxation terms ( $\mu = 0$ ). Then relaxation terms are considered and are assumed stiff. In other word, the mechanical equilibrium solution is obtained at the end of the second step. It can be proved by asymptotic analysis that such strategy yields precisely to System (2) (see [44] Appendix B for the details).

Numerical resolution of the pressure non-equilibrium model in the limit of stiff pressure relaxation is then addressed. In regular zones, this model is self consistent. But in the presence of shocks the internal energy equations are inappropriate. To correct the thermodynamic state predicted by these equations in the presence of shocks, the total mixture energy equation is used. This correction is valid on both sides of the interface, when the flow tends to the single phase limit. The details of this correction will be examined further. For now, the pressure non-equilibrium system (6) is augmented by the redundant equation (7).

### 3.1. Hyperbolic solver

The hyperbolic solver is aimed to solve System (6-7) in the absence of relaxation terms ( $\mu = 0$ ). The first ingredient corresponds to the Riemann solver used to compute the fluxes that cross each cell boundary. Then the variables are updated with a Godunov type method.

#### 3.1.1. HLLC Riemann solver

The [51] solver is considered at cell boundaries, separating left (L) and right (R) states. This solver involves 3 waves, is genuinely positive and valid for any convex equation of state. It is thus an excellent candidate for the various applications we are dealing with. The left- and right-facing waves speeds are readily obtained, following [10] estimates,

$$S_R = \max(u_L + c_L, u_R + c_R), \quad S_L = \min(u_L - c_L, u_R - c_R),$$

where the sound speed still obeys the frozen sound speed relation,  $c_{R,L}^2 = Y_{1R,L}c_{1R,L}^2 + Y_{2R,L}c_{2R,L}^2$ . The intermediate wave speed is estimated under HLL approximation,

$$S_M = \frac{(\rho u^2 + p)_L - (\rho u^2 + p)_R - S_L(\rho u)_L + S_R(\rho u)_R}{(\rho u)_L - (\rho u)_R - S_L\rho_L + S_R\rho_R},$$

with the mixture density and mixture pressure defined previously.

From these wave speeds, the following variable states are determined,

$$(\alpha_k \rho_k)_R^* = (\alpha_k \rho_k)_R \frac{S_R - u_R}{S_R - S_M}, \quad (\alpha_k \rho_k)_L^* = (\alpha_k \rho_k)_L \frac{S_L - u_L}{S_L - S_M},$$

$$p^* = p_R + \rho_R u_R (u_R - S_R) - \rho_R^* S_M (S_M - S_R),$$

with  $\rho_{R,L}^* = (\alpha_1 \rho_1)_{R,L}^* + (\alpha_2 \rho_2)_{R,L}^*$  and,

$$E_R^* = \frac{\rho_R E_R (u_R - S_R) + p_R u_R - p^* S_M}{\rho_R^* (S_M - S_R)}, \quad E_L^* = \frac{\rho_L E_L (u_L - S_L) + p_L u_L - p^* S_M}{\rho_L^* (S_M - S_L)},$$

with  $E = Y_1 e_1 + Y_2 e_2 + \frac{1}{2} u^2$ . The upperscript '\*' stands for the Riemann problem solution states.

The volume fraction jump is readily obtained, as in the absence of relaxation effects the volume fraction is constant along fluid trajectories,

$$\alpha_{kR}^* = \alpha_{kR}, \quad \alpha_{kL}^* = \alpha_{kL}.$$

As the volume fraction is constant across left- and right-facing waves, the fluid density is determined from the preceding relations:

$$\rho_{kR,L}^* = \rho_{kR,L} \frac{u_{R,L} - S_{R,L}}{S_M - S_{R,L}}$$



Internal energy jumps are determined with the help of approximate Hugoniot relations for System (6). Let us consider the example of fluids governed by the stiffened gas EOS (3). With the help of the EOS, the phasic pressures are constrained along their Hugoniot curves as functions only of the corresponding phase density,

$$p_{kR,L}^*(\rho_{kR,L}^*) = (p_{kR,L} + p_{\infty k}) \frac{(\gamma_k - 1)\rho_{kR,L} - (\gamma_k + 1)\rho_{kR,L}^*}{(\gamma_k - 1)\rho_{kR,L}^* - (\gamma_k + 1)\rho_{kR,L}} - p_{\infty k}$$

The phases internal energies are then determined from the EOS:  $e_{kR,L}^* = e_{kR,L}^*(p_{kR,L}^*, \rho_{kR,L}^*)$ . Equipped with this solver, the next step is to develop a Godunov type scheme.

### 3.1.2. Godunov type method

In the absence of relaxation terms, the conservative part of System (6) is updated with the conventional Godunov scheme:

$$U_i^{n+1} = U_i^n - \frac{\Delta t}{\Delta x} (F^*(U_i^n, U_{i+1}^n) - F^*(U_{i-1}^n, U_i^n))$$

with  $U = ((\alpha\rho)_k, \rho u, \rho E)^T$  and  $F = ((\alpha\rho)_k u, (\rho u + (\alpha_1 p_1 + \alpha_2 p_2)), (\rho E + (\alpha_1 p_1 + \alpha_2 p_2)) u)^T$ . The volume fraction equation is updated with the Godunov method for advection equations:

$$\alpha_{ki}^{n+1} = \alpha_{ki}^n - \frac{\Delta t}{\Delta x} \left( (u\alpha_k)_{i+1/2}^* - (u\alpha_k)_{i-1/2}^* - \alpha_{ki,l}^n (u_{i+1/2}^* - u_{i-1/2}^*) \right)$$

This scheme guarantees volume fraction positivity during the hyperbolic step. Obviously, higher order extension of the Godunov method can be considered.

Regarding the non-conservative energy equations, there is no hope to determine accurate numerical approximation in the presence of shocks [21]. Therefore, we use the simplest approximation of the corresponding equations by assuming the product  $(\alpha p)_{k,i}^n$  constant during the time step:

$$(\alpha p e)_{k,i}^{n+1} = (\alpha p e)_{k,i}^n - \frac{\Delta t}{\Delta x} \left( (\alpha p e u)_{k,i+1/2}^* - (\alpha p e u)_{k,i-1/2}^* + (\alpha p)_{k,i}^n (u_{i+1/2}^* - u_{i-1/2}^*) \right)$$

The lack of accuracy in the internal energy computation resulting from the present scheme is not so crucial. The internal energies will be used only to estimate the phases pressures at the end of the hyperbolic step, before the relaxation one. The relaxation step will give a first correction to the internal energies, in agreement with the second law of thermodynamics. A second correction will be made with the help of the total mixture energy. The details of these two steps are described in the next subsections.

## 3.2. Relaxation step

This step is of major importance to fulfill interface conditions in non-uniform velocity and pressure flow conditions. It also forces the solution of the pressure non-equilibrium model (6) to converge to that of the

equilibrium model (2). In the relaxation step the system to consider reads,

$$\left\{ \begin{array}{l} \frac{\partial \alpha_1}{\partial t} = \mu (p_1 - p_2), \\ \frac{\partial \alpha_1 \rho_1}{\partial t} = 0, \\ \frac{\partial \alpha_2 \rho_2}{\partial t} = 0, \\ \frac{\partial \rho u}{\partial t} = 0 \\ \frac{\partial \alpha_1 \rho_1 e_1}{\partial t} = -p_I \mu (p_1 - p_2), \\ \frac{\partial \alpha_2 \rho_2 e_2}{\partial t} = p_I \mu (p_1 - p_2), \\ \frac{\partial \rho E}{\partial t} = 0 \end{array} \right. \quad (8)$$

in the limit  $\mu \rightarrow +\infty$ .

After some manipulations the internal energy equations become:

$$\frac{\partial e_k}{\partial t} + p_I \frac{\partial v_k}{\partial t} = 0$$

This system can be written in integral form as,

$$e_k - e_k^0 + \hat{p}_{Ik}(v_k - v_k^0) = 0$$

with  $\hat{p}_{Ik} = \frac{1}{v_k - v_k^0} \int_0^{\Delta t} p_I \frac{\partial v_k}{\partial t} dt$ .

Determination of pressure averages has to be done in agreement with thermodynamic considerations.

By summing the internal energy equations we have:

$$\sum_k (Y_k e_k - Y_k e_k^0) + \sum_k \hat{p}_{Ik} (Y_k v_k - Y_k v_k^0) = 0$$

As the system conserves energy,  $\sum_k (Y_k e_k - Y_k e_k^0) = 0$ .

On the other hand, mass conservation implies,  $\sum_k (Y_k v_k - Y_k v_k^0) = 0$ .

Therefore, the identity,

$$\sum_k (Y_k e_k - Y_k e_k^0) + \sum_k \hat{p}_{Ik} (Y_k v_k - Y_k v_k^0) = 0$$

is fulfilled if the various pressure averages are taken equal, i.e.,

$$\hat{p}_{Ik} = \hat{p}_I = p.$$

This pressure average estimate also agrees with the entropy inequality. The system to solve is thus composed of equations,

$$e_k(p, v_k) - e_k^0(p_k^0, v_k^0) + \hat{p}_I(v_k - v_k^0) = 0, \quad \text{for } k = 1, 2 \quad (9)$$

which involves 2+1 unknowns,  $v_k$  ( $k = 1, 2$ ) and  $p$ . Its closure is achieved by the saturation constraint,

$$\sum_k \alpha_k = 1,$$

that is rewritten under the form,

$$\sum_k (\alpha \rho)_k v_k(p) = 1. \quad (10)$$

As the  $(\alpha \rho)_k$  are constant during the relaxation process, this system is replaced by a single equation with a single unknown ( $p$ ). With the help of the EOS (3) the energy equations (9) become,

$$v_k(p) = v_k^0 \frac{p_k^0 + \gamma_k p_{\infty k} + (\gamma_k - 1) \hat{p}_I}{p + \gamma_k p_{\infty k} + (\gamma_k - 1) \hat{p}_I}$$

and thus the only equation to solve (for  $p$ ) is (10).

Once the relaxed pressure is found, the phases specific volumes and volume fractions are determined. However, there is no guarantee that the mixture EOS or the mixture energy be in agreement with this relaxed pressure. In order to respect total energy and correct shock dynamics on both sides of the interface, the following correction is employed.

### 3.3. Reset step

As the volume fractions have been estimated previously by the relaxation method, the mixture pressure can be determined from the mixture EOS based on the mixture energy which is known from the solution of the total energy equation. As the mixture total energy obeys a conservation law, its evolution is accurate in the entire flow field and in particular at shocks.

Again considering fluids governed by the stiffened gas EOS, the mixture EOS is given by (4). This EOS is valid in pure fluids and in the diffuse interface zone. As it is valid in pure fluids and based on the total energy equation, it guarantees correct wave dynamics on both sides of the interface. Inside the numerical diffusion zone of the interface, numerical experiments show that the method is accurate too, as the volume fractions used in the mixture EOS have a quite accurate prediction from the relaxation step.

To summarise, the pressure at the end of the time step is computed with the mixture EOS (4) as:

$$p^{n+1} = p(\rho^{n+1}, e^{n+1}, \alpha_k^{relax}), \quad (11)$$

where  $\rho^{n+1}$  and  $e^{n+1}$  represent respectively the mixture density and mixture internal energy at time  $t^{n+1}$ , while  $\alpha_k^{relax}$  represent the volume fractions determined at the end of the relaxation step. Once the mixture pressure is determined the internal energies of the phases are reset with the help of their respective EOS before going to the next time step,

$$e_k^{n+1} = e_k(p^{n+1}, \alpha_k \rho_k^{n+1}, \alpha_k^{n+1}), \quad (12)$$

where the volume fractions at the new time correspond to those determined at the end of the relaxation step ( $\alpha_k^{n+1} = \alpha_k^{relax}$ ).

### 3.4. Shock propagation in multiphase mixture

When the flow involves material interfaces only, the preceding algorithm is particularly simple and efficient. But in some situations, physical mixtures of materials are under interest, eventually in the presence of shocks. This occurs for example in the study of shocks and detonation waves in heterogeneous materials. In this situation, the shock energy has to be apportioned correctly among the phases; otherwise the shock speeds as well as the various jumps are incorrect. The goal is thus to impose the shock conditions (5) in the pressure equilibrium solution. This issue has been addressed in [34] and a solution method was given in [36]. It consists in replacing Equations (9) in the previous pressure relaxation step by,

$$e_k(p, v_k) - e_k^0(p_k^0, v_k^0) + \frac{p + p_0}{2}(v_k - v_k^0) = 0, \quad \text{for } k = 1, 2 \quad (13)$$

where the state with superscript 0 indicates the Hugoniot pole. This state has to be constant inside the shock layer. To do this, additional evolution equations are used to replace the internal energy equations of System (6), in the shock layer only. These equations read:

$$\begin{cases} \frac{\partial v_k^0}{\partial t} + u \frac{\partial v_k^0}{\partial x} = 0, & \text{for } k = 1, 2 \\ \frac{\partial p_0}{\partial t} + u \frac{\partial p_0}{\partial x} = 0 \end{cases} \quad (14)$$

Thanks to (13) and (14) the method converges to the correct shock state.

### 3.5. Summary of the numerical method

The numerical method can be summarized as follows:

- At each cell boundary, solve the Riemann problem of System (6) in the absence of relaxation terms with the HLLC solver or any positive Riemann solver.
- Evolve all flow variables with the Godunov method or higher order extensions.
- Determine the relaxed pressure and especially the volume fraction by solving Equation (10) with the help of the Newton method. Equations (9) are used if interfaces separate pure fluids. If one of the media corresponds to a multiphase mixture, Equations (9) are replaced by (13). In this instance, (14) have to be solved in the shock layer. The shock layer is detected thanks to shock indicators such as [50] (see paragraph 14.6.4) or [28].
- Compute the mixture pressure with Equation (4).
- Reset the internal energies with the computed pressure with the help of their respective EOS (12).
- Go to the first item for the next time step.

### 3.6. Computational example

A non-conventional computational example is shown in the Figure 2. A piston impacts a liquid column with a curved liquid-gas interface. A Richtmyer-Meshkov type instability appears, as expected. Unexpected features appear too, as cavitation pockets are created in the liquid domain, due to liquid jet presence. To deal with such a flow, the model has to deal with material interfaces, shocks and expansions waves. It must also predict dynamic interfaces appearance. Cavitation pockets are here consequences of the small amount of gas present in the liquid that grows under expansion effects as a result of the pressure equilibrium condition.

On the basis of the [22] model, several extensions have been done. Some of them are summarized in the rest of the paper.

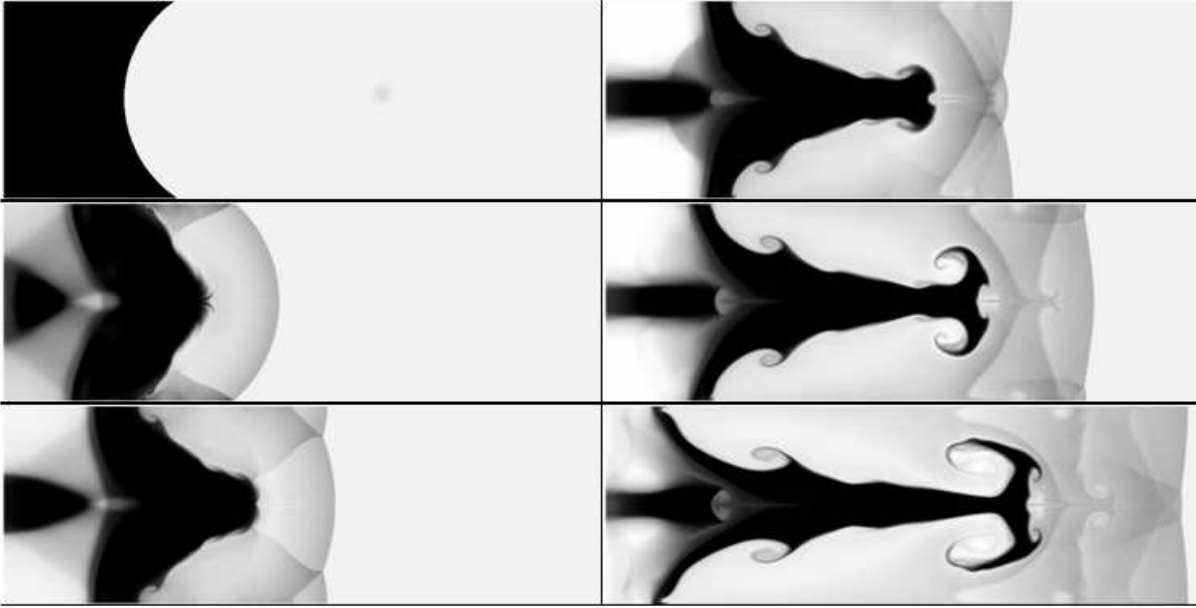


FIGURE 2. Richmyer-Meshkov instability with a cavitating liquid and a non miscible gas.

#### 4. CAPILLARY EFFECTS

The following capillary flow model is a slight variation of the [33] model where the CSF method of [5] was embedded in the compressible Kapila model. The corresponding system reads:

$$\left\{ \begin{array}{l}
 \frac{\partial \alpha_1}{\partial t} + \vec{u} \cdot \vec{\nabla} \alpha_1 - \frac{(\rho_2 c_2^2 - \rho_1 c_1^2)}{\frac{\rho_1 c_1^2}{\alpha_1} + \frac{\rho_2 c_2^2}{\alpha_2}} \operatorname{div}(\vec{u}) = 0, \quad \text{for } k = 1, 2 \\
 \\
 \frac{\partial \rho Y_1}{\partial t} + \operatorname{div}(\rho Y_1 \vec{u}) = 0 \\
 \\
 \frac{\partial \rho}{\partial t} + \operatorname{div}(\rho \vec{u}) = 0 \\
 \\
 \frac{\partial \rho \vec{u}}{\partial t} + \operatorname{div} \left[ P \vec{I} + \rho \vec{u} \otimes \vec{u} - \sigma \left( |\vec{\nabla} Y_1| \vec{I} - \frac{\vec{\nabla} Y_1 \otimes \vec{\nabla} Y_1}{|\vec{\nabla} Y_1|} \right) \right] = \vec{0} \\
 \\
 \frac{\partial \rho \left( e + \frac{\sigma |\vec{\nabla} Y_1|}{\rho} + \frac{1}{2} \|\vec{u}\|^2 \right)}{\partial t} + \operatorname{div} \left[ \left( \rho \left( e + \frac{\sigma |\vec{\nabla} Y_1|}{\rho} + \frac{1}{2} \|\vec{u}\|^2 \right) + P \right) \vec{u} - \sigma \left( |\vec{\nabla} Y_1| \vec{I} - \frac{\vec{\nabla} Y_1 \otimes \vec{\nabla} Y_1}{|\vec{\nabla} Y_1|} \right) \cdot \vec{u} \right] = 0
 \end{array} \right. \quad (15)$$

Where  $\sigma$  represents the surface tension coefficient.

This formulation presents at least two advantages:

- Compressible effects are present in conjunction to surface tension ones.

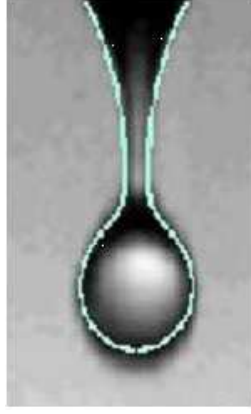


FIGURE 3. Comparison of computed drop formation under gravity effects (light lines) versus experimental photograph (grey contours). System (15) is solved everywhere, in pure liquid, pure gas and at the interface.

- There is no interface width, compared to the [6] second gradient theory that needs too fine resolution for practical applications.

A computation example and comparison with experiments is shown in the Figure 3. At the discrete level, when capillary effects are considered, care has to be done with the following specific points:

- The pressure is no longer constant at the contact discontinuity. The local interface curvature and surface tension effects are accounted for in the Riemann solver. Details are given in [33].
- Capillary effects cannot be activated with initial discontinuities in the mass fractions. Thus, the first computational time steps (less than 10) are achieved without surface tension, in order that artificial smearing render discrete mass fraction gradients available.

## 5. PHASE TRANSITION

This extension has been done in [43] on the basis of entropy production examination. In the absence of capillary effects, the resulting system reads,

$$\left\{ \begin{array}{l} \frac{\partial \alpha_1}{\partial t} + \vec{u} \cdot \vec{\nabla}(\alpha_1) = \frac{(\rho_2 c_2^2 - \rho_1 c_1^2)}{\frac{\rho_1 c_1^2}{\alpha_1} + \frac{\rho_2 c_2^2}{\alpha_2}} \operatorname{div}(\vec{u}) + \rho \nu (g_2 - g_1) \frac{\frac{c_1^2}{\alpha_1} + \frac{c_2^2}{\alpha_2}}{\frac{\rho_1 c_1^2}{\alpha_1} + \frac{\rho_2 c_2^2}{\alpha_2}} + H(T_2 - T_1) \frac{\frac{\Gamma_1}{\alpha_1} + \frac{\Gamma_2}{\alpha_2}}{\frac{\rho_1 c_1^2}{\alpha_1} + \frac{\rho_2 c_2^2}{\alpha_2}} \\ \frac{\partial \alpha_1 \rho_1}{\partial t} + \operatorname{div}(\alpha_1 \rho_1 \vec{u}) = \rho \nu (g_2 - g_1) \\ \frac{\partial \alpha_2 \rho_2}{\partial t} + \operatorname{div}(\alpha_2 \rho_2 \vec{u}) = -\rho \nu (g_2 - g_1) \\ \frac{\partial \rho \vec{u}}{\partial t} + \operatorname{div}(\rho \vec{u} \otimes \vec{u}) + \vec{\nabla}(p) = 0 \\ \frac{\partial \rho E}{\partial t} + \operatorname{div}((\rho E + p) \vec{u}) = 0 \end{array} \right. \quad (16)$$

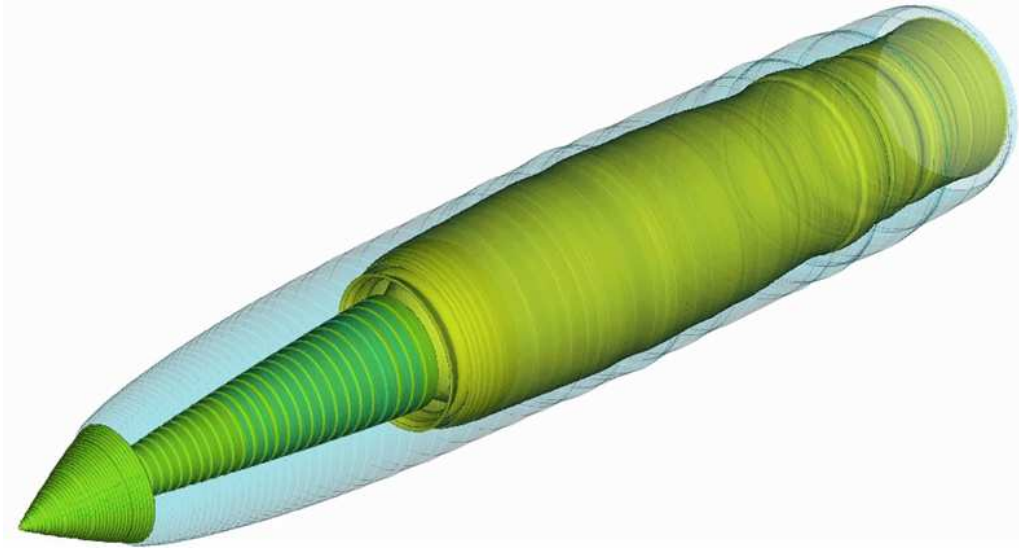


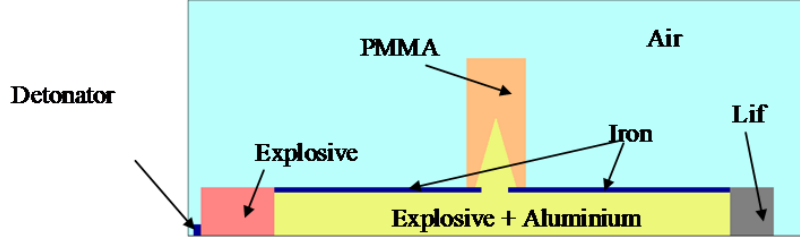
FIGURE 4. Cavitating flow around a hypervelocity underwater missile. Combustion gases are shown in yellow contours and are in contact with vapour, in blue colour. The vapour is separated from the liquid (not shown) by an evaporating interface. Two different types of interfaces are thus present in this example. The results are issued from [35].

with the following notations:  $g_k = h_k - T_k s_k$  represents the Gibbs free energy,  $H$  represents the temperature relaxation parameter and  $\nu$  the mass transfer kinetics.

Some comments are due regarding the volume fraction equation. The first term in the right hand side, present in the [22] model, represents mechanical relaxation effects, present in all zones where the velocity divergence is non zero (shocks, compressions, expansions). The second term represents volume variations due to mass transfer, in a context where both phases are compressible. The last group of terms represents dilatation effects due to heat transfer.  $\Gamma_k$  represents the Gruneisen coefficient of the phase  $k$ .

The model needs thermodynamic parameters on one hand and kinetics ones, such as  $H$  and  $\nu$  on the other hand. In the present formulation, each fluid has its own thermodynamics and the equation of state parameters are determined on the basis of the phase diagram, as detailed in [26]. Regarding kinetic parameters, we have learnt in the beginning of this paper that it was possible to fulfill interface conditions of simple contact by using infinite mechanical relaxation parameters. Here, infinite thermal and mass transfer kinetics are used (infinite  $H$  and  $\nu$ ). It means that local thermodynamic equilibrium is assumed. This renders possible the consideration of phase transition fronts propagating at global finite rate [43]. It is shown in this reference that phase transition fronts propagate in metastable liquids at the characteristic speed of the full equilibrium system. This is indeed the system that is solved at the evaporating interface. It consists in the mixture mass, momentum and energy equations, closed by pressure, temperature and Gibbs free energy equilibrium conditions. The associated sound speed is very low and the lower CJ point conditions [7, 8, 48, 49] merge with the aforementioned characteristic speeds.

Infinite heat and mass transfer kinetic parameters have been used in the example shown in Figure 4 at liquid-vapour interfaces when the liquid is overheated (metastable). At vapour-non condensable gas interfaces, the same kinetic parameters have been set to zero, in order to fulfill contact interface conditions.



## 6. DETONATIONS

To deal with the detonation of condensed energetic materials, possibly heterogeneous, the same flow model as previously can be used except regarding the equations of state that must contain appropriate reference energy yielding exothermic heat of reaction. For example, the stiffened gas equation of state (3) now expresses as,

$$p_k = (\gamma_k - 1)\rho_k(e_k - q_k) - \gamma_k p_{\infty k}$$

where  $q_k$  represents the reference energy.

It is then necessary to use finite rate heat and mass transfer coefficients, respectively  $H$  and  $\nu$ . Let us present first an illustrative example. A detonation tube is filled with a heterogeneous explosive mixture. A shock wave is emitted by a detonator and transforms to a detonation that propagates in the explosive, loaded with aluminium particles.

Material interfaces are present too as 7 different materials have to be considered. As previously mentioned, the same equations are solved everywhere with the same flow solver. The results shown in the Figure 5 are taken from [36]. Starting from the flow model expressed in Section 5, it is possible to determine generalized Chapman Jouguet relations, yielding non-ideal detonation behaviour even in pure 1D planar flow configuration. Indeed, expressing the flow model between the shock front and the sonic surface, in the detonation wave frame of reference, the following expression for the velocity divergence is obtained:

$$\frac{d\bar{u}}{dx} = \frac{1}{\rho(c^2 - \bar{u}^2)} \left\{ \frac{\Gamma_1 \Gamma_2}{\alpha_1 \alpha_2} \frac{\left( \frac{\rho_2 c_2^2}{\Gamma_2} - \frac{\rho_1 c_1^2}{\Gamma_1} \right)}{\left( \frac{\rho_1 c_1^2}{\alpha_1} + \frac{\rho_2 c_2^2}{\alpha_2} \right)} H(T_2 - T_1) \right. \\ \left. + \left( \frac{\left( \frac{\rho_2 c_2^2}{\Gamma_2} - \frac{\rho_1 c_1^2}{\Gamma_1} \right)}{\left( \frac{\rho_1 c_1^2}{\alpha_1} + \frac{\rho_2 c_2^2}{\alpha_2} \right)} \left( \frac{c_1^2}{\alpha_1} + \frac{c_2^2}{\alpha_2} \right) + h_2 - \frac{c_2^2}{\Gamma_2} - \left( h_1 - \frac{c_1^2}{\Gamma_1} \right) \right) \frac{\dot{m}_1}{\left( \frac{\alpha_1}{\Gamma_1} + \frac{\alpha_2}{\Gamma_2} \right)} \right\}$$

The generalized Chapman Jouguet relation appears immediately. On the sonic surface characterized by,

$$\bar{u} = c,$$



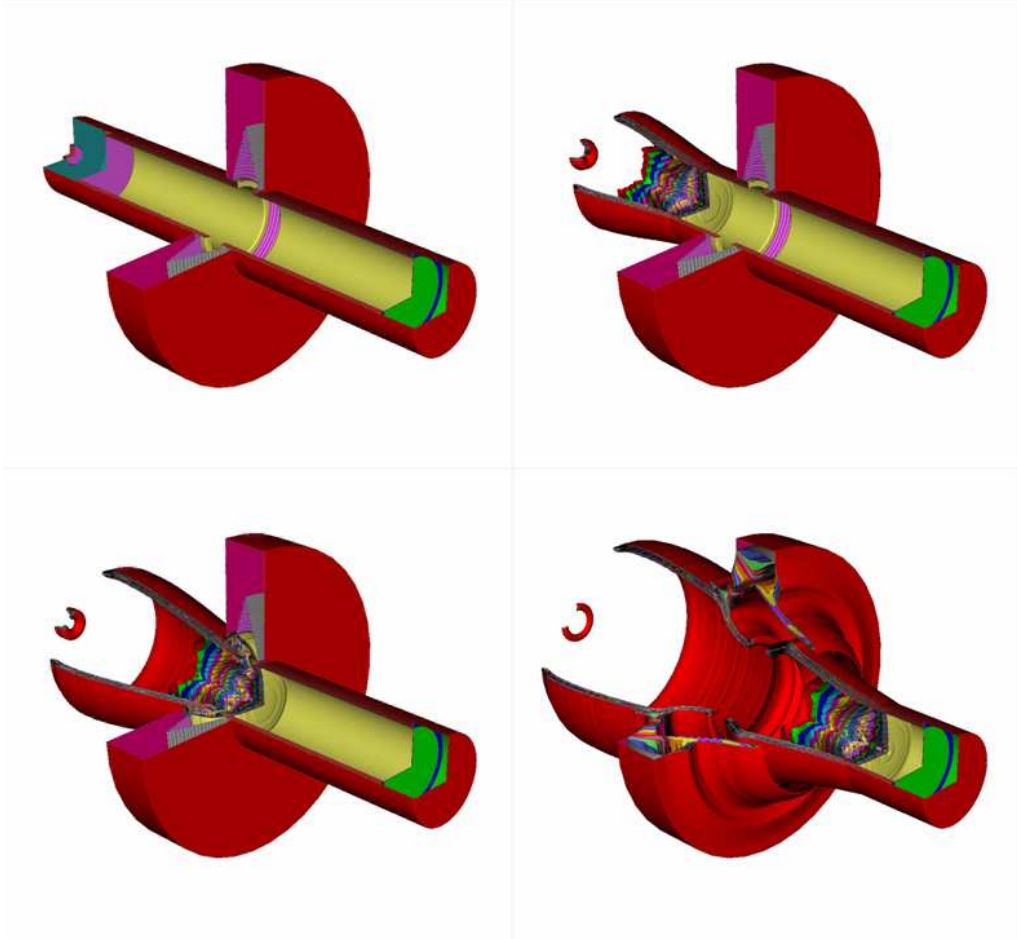


FIGURE 5. Mixture density contours at the initial time and at three successive times showing detonation dynamics and interfaces motion for the detonation tube problem.

necessarily,

$$\frac{\Gamma_1 \Gamma_2}{\alpha_1 \alpha_2} \frac{\left( \frac{\rho_2 c_2^2}{\Gamma_2} - \frac{\rho_1 c_1^2}{\Gamma_1} \right)}{\left( \frac{\rho_1 c_1^2}{\alpha_1} + \frac{\rho_2 c_2^2}{\alpha_2} \right)} H(T_2 - T_1) + \left( \frac{\left( \frac{\rho_2 c_2^2}{\Gamma_2} - \frac{\rho_1 c_1^2}{\Gamma_1} \right)}{\left( \frac{\rho_1 c_1^2}{\alpha_1} + \frac{\rho_2 c_2^2}{\alpha_2} \right)} \left( \frac{c_1^2}{\alpha_1} + \frac{c_2^2}{\alpha_2} \right) + h_2 - \frac{c_2^2}{\Gamma_2} - \left( h_1 - \frac{c_1^2}{\Gamma_1} \right) \right) \frac{\dot{m}_1}{\left( \frac{\alpha_1}{\Gamma_1} + \frac{\alpha_2}{\Gamma_2} \right)} = 0$$

Thus, when heat transfers are absent the conventional CJ relation is recovered:  $\dot{m}_1 = 0$  when  $\bar{u} = c$ . These extended CJ relations have non trivial consequences. While the CJ detonation velocity is considered as the maximum admissible detonation speed, heterogeneous explosives can overpass this limit. This theoretical fact has been checked by [3] on the basis of experiments done at Sarov in Russia, with the help of various liquid explosive mixtures loaded with inert solid particles. The heat transfers are not responsible for the increase

in detonation velocity. The explanation comes from the fact that, in temperature non-equilibrium conditions the phases have unconstrained dilatation. Indeed, due to the fast phenomenon occurring in the reaction zone and due to the quite large particle sizes, thermal equilibrium assumed in conventional CJ and ZND models is not justified and yields to underestimated detonation speeds, as a consequence of constrained dilatation of the various substances.

The present flow model, CJ conditions and ZND structure have been recently investigated in details by [46] for the study of highly non-ideal ammonium nitrate explosives, showing in particular impressive comparison with experimental detonation records in a broad range of confinements and wide range of charge diameters.

Let's now turn back to the issue of kinetic coefficients determination ( $H$  and  $\nu$ ). In drastic flow conditions occurring in detonations, it is not possible to determine by direct measurements such parameters. In [3], analysing detonation experiments based on explosive liquids loaded with particles of different sizes, from 0.1 to 100  $\mu m$  it appeared that heat exchanges are negligible ( $H=0$ ). This is due to the short particle life time in the detonation reaction zone. In [46] an inverse method based on detonation front curvature is given, allowing accurate determination of the decomposition rate kinetics  $\nu$ . The method given in this reference is a 2D extension of the well known [54] streamline method for curved detonation waves, widely used to find decomposition kinetics of explosives.

## 7. PERSPECTIVES

Diffuse interface methods are now mature enough to deal with realistic and advanced applications. There are however many fundamental issues to address:

- The shock relations (5) have been demonstrated for weak shocks. They have been compared to experimental data for strong shocks (in the megabar range) showing excellent agreement too [42]. However, there is a lack of mathematical proof for strong shocks.
- The numerical method summarized in Section 3 and its variants [32] are very efficient for high speed flows. However, many applications deal with low Mach number flow conditions and there is a clear need for efficient algorithms at all Mach number for diffuse interface models. Efforts in this direction have been done by [24].
- Another numerical issue deals with long time evolutions, where interfaces become too smeared with upwind scheme computations. There is thus a clear need to sharpen interfaces without losing conservation properties.
- There are also extra mathematical modelling issues when dealing with extra physics extensions, such as for example, hot spot modelling in shock to detonation transition in the area of combustion, solid fluid coupling [12] to make a bridge between fluid and solid mechanics, the direct numerical simulation of boiling flows in the area of energetics.
- Another important modelling issue is related to velocity drift effects restoration in diffuse interface formulations. Attempts in this direction have been done by [18], [38] and [40].

The first author is particular grateful to Stéphane Gerbi and Christian Bourdarias for their kind invitation at the AMIS 2012 conference in Chambéry.

## REFERENCES

- [1] R. Abgrall and R. Saurel. Discrete equations for physical and numerical compressible multiphase mixtures. *Journal of Computational Physics*, 186(2):361–396, 2003.
- [2] M. Baer and J. Nunziato. A two-phase mixture theory for the deflagration-to-detonation transition (DDT) in reactive granular materials. *Int. J. of Multiphase Flows*, 12:861–889, 1986.
- [3] G. Baudin, A. Lefrançois, R. Saurel, F. Petitpas, O. Le Metayer, J. Massoni, V. M. Belski, and E. Zotov. Toward a thermal disequilibrium multi-phase model for high explosives containing metallic particles. *Journal of Energetic Materials*, 28:154–179, 2010.

- [4] D. Benson. Computational methods in Lagrangian and Eulerian hydrocodes. *Computer method in Applied Mechanics and Engineering*, 99:235–394, 1992.
- [5] J. Brackbill, D. Kothe, and C. Zemach. A continuum method for modelling surface tension. *Journal of Computational Physics*, 100:335–354, 1992.
- [6] J. Cahn and J. Hilliard. Free energy of a nonuniform system i: Interfacial free energy. *J. Chem. Physics*, 28(2):258, 1958.
- [7] H. Chaves. Changes of phase and waves on depressurization of liquids with high specific heat. *Mitt. Max-Planck-Institut f. Strömungsforschung*, 77, 1984.
- [8] H. Chaves. Phasenübergänge und wellen bei der entspannung von fluiden hoher spezifischer warme. *Mitt. Max-Planck-Institut f. Strömungsforschung*, 77, 1984.
- [9] A. Chinnayya, E. Daniel, and R. Saurel. Computation of detonation waves in heterogeneous energetic materials. *Journal of Computational Physics*, 196:490–538, 2004.
- [10] S. F. Davis. Simplified second order Godunov type methods. *SIAM J. Sci. Comp.*, 9:445–473, 1988.
- [11] C. Farhat and F. Roux. A method for finite element tearing and interconnecting and its parallel solution algorithm. *International Journal for Numerical methods in Engineering*, 32:457–492, 1991.
- [12] N. Favrie, S. Gavriluk, and R. Saurel. Solid-fluid diffuse interface model in cases of extreme deformations. *Journal of Computational Physics*, 228(16):6037–6077, 2009.
- [13] R. Fedkiw, T. Aslam, B. Merriman, and S. Osher. A non oscillatory Eulerian approach to interfaces in multimaterial flows (The Ghost Fluid Method). *Journal of Computational Physics*, 152:457–492, 1999.
- [14] S. Gavriluk and R. Saurel. A compressible multiphase flow model with microinertia. *Journal of Computational Physics*, 175:326–360, 2002.
- [15] J. Glimm, J. Grove, X. Li, K. Shyue, Q. Zhang, and Y. Zeng. Three dimensional front tracking. *SIAM J. Scientific Computing*, 19:703–727, 1998.
- [16] S. Godunov. A finite difference method for numerical computation of discontinuous solutions of the equations of fluid dynamics. *Math Sb.*, 47:357–393, 1959.
- [17] D. Gueyffier, L. Li, A. Nadim, R. Scardovelli, and S. Zaleski. Volume-of-fluid interface tracking with smoothed surface stress methods for three-dimensional flows. *Journal of Computational Physics*, 152:423–456, 1999.
- [18] H. Guillard and F. Duval. A darcy law for the drift velocity in a two-phase flow model. *Journal of Computational Physics*, 224:288–313, 2007.
- [19] C. Hirt, A. Amsden, and J. Cook. An arbitrary Lagrangian Eulerian computing method for all flow speeds. *Journal of Computational Physics*, 14:227–253, 1974.
- [20] C. Hirt and B. Nichols. Volume of fluid (vof) method for the dynamics of free boundaries. *Journal of Computational Physics*, 39:201–255, 1981.
- [21] T. Hou and P. Le Floch. Why non-conservative schemes converge to the wrong solution: Error analysis. *Math. Comp.*, 62:497–530, 1994.
- [22] A. Kapila, R. Menikoff, J. Bdzil, S. Son, and D. Stewart. Two-phase modeling of DDT in granular materials: Reduced equations. *Physics of Fluids*, 13:3002–3024, 2001.
- [23] S. Karni. Multicomponent flow calculations by a consistent primitive algorithm. *Journal of Computational Physics*, 112:31–43, 1994.
- [24] S. Le Martelot, B. Nkonga, and R. Saurel. Liquid and liquid-gas flows at all speeds: Reference solutions and numerical schemes. *Journal of Computational Physics, in revision*, 2013.
- [25] S. Le Martelot, R. Saurel, and B. Nkonga. Towards the direct numerical simulation of nucleate boiling flows. *Progress in Energy and Combustion Science, in preparation*, 2013.
- [26] O. Le Metayer, J. Massoni, and R. Saurel. Elaborating equations of state of a liquid and its vapor for two-phase flow models. *Int. J. of Thermal Sciences*, 43:265–276, 2004.
- [27] R. Leveque and K. Shyue. Two-dimensional front tracking based on high resolution wave propagation methods. *Journal of Computational Physics*, 123(2):354–368, 1996.
- [28] R. Menikoff and M. Shaw. Reactive burn models and ignition and growth concept. *Los Alamos National Laboratory Report*, LA-UR-10-01870, 2010.
- [29] G. Miller and E. Puckett. A high-order Godunov method for multiple condensed phases. *Journal of Computational Physics*, 128(1):134–164, 1996.
- [30] W. Mulder, S. Osher, and J. Sethian. Computing interface motion: The compressible Rayleigh-Taylor and Kelvin-Helmholtz instabilities. *Journal of Computational Physics*, 100:209, 1992.
- [31] S. Osher and R. Fedkiw. Level set methods: An overview and some recent results. *Journal of Computational Physics*, 169:463–502, 2001.
- [32] M. Pelanti and K. Shyue. A mixture energy consistent 6-equation two-phase model for fluids with interfaces and cavitation phenomena. *Conference Applied Math. In Savoie (AMIS 2012), 19-22 june 2012, Chambéry, France*, 2012.
- [33] G. Perigaud and R. Saurel. A compressible flow model with capillary effects. *J. Comp. Phys.*, 209:139–178, 2005.
- [34] F. Petitpas, E. Franquet, R. Saurel, and O. Le Metayer. A relaxation-projection method for compressible flows. Part 2: Artificial heat exchange for multiphase shocks. *Journal of Computational Physics*, 225(2):2214–2248, 2007.

- [35] F. Petitpas, J. Massoni, R. Saurel, E. Lapebie, and L. Munier. Diffuse interface models for high speed cavitating underwater systems. *Int. J. of Multiphase Flows*, 35(8):747–759, 2009.
- [36] F. Petitpas, R. Saurel, E. Franquet, and A. Chinnayya. Modelling detonation waves in condensed energetic materials: Multiphase CJ conditions and multidimensional computations. *Shock waves*, 19(5):377–401, 2009.
- [37] R. Saurel and R. Abgrall. A multiphase Godunov method for compressible multifluid and multiphase flows. *Journal of Computational Physics*, 150:425–467, 1999.
- [38] R. Saurel, N. Favrie, F. Petitpas, M. Lallemand, and S. Gavriluk. Modeling dynamic and irreversible powder compaction. *Journal of Fluid Mechanics*, 664:348–396, 2010.
- [39] R. Saurel, S. Gavriluk, and F. Renaud. A multiphase model with internal degrees of freedom: Application to shock-bubble interaction. *Journal of Fluid Mechanics*, 495:283–321, 2003.
- [40] R. Saurel, G. Huber, G. Jourdan, E. Lapebie, and L. Munier. Modelling spherical explosions with turbulent mixing and post-combustion. *Physics of Fluids*, 24:115101–42, 2012.
- [41] R. Saurel and O. Le Metayer. A multiphase model for compressible flows with interfaces, shocks, detonation waves and cavitation. *Journal of Fluid Mechanics*, 431:239–271, 2001.
- [42] R. Saurel, O. Le Metayer, J. Massoni, and S. Gavriluk. Shock jump relations for multiphase mixtures with stiff mechanical relaxation. *Shock Waves*, 16:209–232, 2007.
- [43] R. Saurel, F. Petitpas, and R. Abgrall. Modelling phase transition in metastable liquids: application to cavitating and flashing flows. *Journal of Fluid Mechanics*, 607:313–350, 2008.
- [44] R. Saurel, F. Petitpas, and R. Berry. Simple and efficient relaxation methods for interfaces separating compressible fluids, cavitating flows and shocks in multiphase mixtures. *Journal of Computational Physics*, 228(5):1678–1712, 2009.
- [45] D. Scheffer and J. Zukas. Practical aspects of numerical simulation of dynamic events: material interfaces. *International Journal of Impact Engineering*, 24(5-6):821–842, 2000.
- [46] S. Schoch, N. Nikiforakis, B. Lee, and R. Saurel. Multi-phase simulation of ammonium nitrate emulsion detonation. *Combustion and Flame*, in press, 2013.
- [47] J. Sethian. Evolution, implementation and application of level set and fast marching methods for advancing fronts. *Journal of Computational Physics*, 169:503–555, 2001.
- [48] J. Simoes-Moreira and J. Shepherd. Evaporation waves in superheated dodecane. *J. Fluid Mech.*, 382:63–86, 1999.
- [49] P. Thompson, H. Chaves, G. Meier, Y. Kim, and H. Speckmann. Wave splitting in a fluid of large heat capacity. *J. Fluid Mech.*, 185:385–414, 1987.
- [50] E. Toro. *Riemann solvers and numerical methods for fluid dynamics*. Springer Verlag, Berlin, 1997.
- [51] E. Toro, M. Spruce, and W. Speares. Restoration of the contact surface in the hll riemann solver. *Shock waves*, 4:25–34, 1994.
- [52] Von Neuman and R. Richtmyer. A method for the numerical calculation of hydrodynamic shocks. *Journal of Applied Physics*, 21:232–237, 1950.
- [53] A. Wood. A textbook of sound. *G. Bell and Sons LTD, London*, 1930.
- [54] W. Wood and J. Kirkwood. Diameter effect in condensed explosives. The relation between velocity and radius of curvature of the detonation wave. *Journal of Chemical Physics*, 22:1920–1924, 1950.